J Polym Res (2014) 21:593
DOI 10.1007/s10965-014-0593-2

ORIGINAL PAPER

Preparation of poly(vinyl acetate-co-dibutyl maleate)/ sodium-montmorillonite nanocomposite via in situ reverse iodine transfer radical polymerization

Mojtaba Farrokhi · Mahdi Abdollahi

Received: 12 July 2014 / Accepted: 16 October 2014 / Published online: 25 October 2014

Abstract Among other controlled radical polymerization techniques, reverse iodine transfer radical polymerization (RITP) has recently been developed for synthesis of polymers with controlled characteristics. In the present work, poly(vinyl acetate-co-dibutyl maleate)/ sodium montmorillonite (Na-MMT) nanocomposites were synthesized via bulk RITP of the vinyl acetate and dibutyl maleate in the presence of Na-MMT, molecular iodine and 2,2′-azobis(isobutyronitryle) (AIBN) at 70 °C. Effect of the Na-MMT loading on the conversion, molecular weight and its distribution were studied by ^{1}H-NMR and GPC analyses respectively. Structure of the nanocomposites was investigated by XRD and TEM analyses. It was found that under similar conditions, conversion, copolymerization rate and molecular weight of the produced copolymers decrease in the presence of Na-MMT especially when the higher loading of nanoclay (5 wt%) is used. Also, molecular weight distribution increased in the presence of clay. It can be attributed to the existence of an interaction between the functional groups in the clay's surface and the reactants as well as probably to the undesirable chain transfer reactions in the presence of nanoclay. Moreover, results showed that conversion and molecular weight of the copolymer increase by increasing iodine amount in a reaction mixture containing nanoclay, verifying again existence of the interaction between the functional groups in the clay's surface and the reactants (I_2 and monomers). The XRD and TEM results indicated that intercalated structure is formed at a low conversion while exfoliated structure can also be formed at a higher conversion.

Keywords Vinyl acetate (VAc) · Dibutyl maleate (DBM) · Reverse iodine transfer radical polymerization (RITP) · Nanocomposite · Synthesis and characterization

Introduction

In the recent decades, much attention has been paid to polymer/ layered silicate nanocomposites as an advanced polymer material because of the enhancement of nanocomposites properties in comparison with the neat polymer [1–4]. Mechanical [5], magnetic and electric properties [6], thermal stability and flame retardancy [7], gas permeation [8] and modulus [9] of a polymer matrix can be modified by adding a relatively low loading of clay. Such improvement in overall properties of nanocomposites is achieved because of high aspect ratio and high strength of these inorganic nanoparticles. Hybrid nanocomposites supply an attractive and versatile platform for emerging high-added-value applications such as photovoltaic cells and light-emitting devices, lithium ion batteries, supercapacitors and biosensors [10]. Moreover, the degree of dispersion of the clay platelets into the matrix determines the structure of nanocomposites and affects the aforementioned properties. Based on the reactants, processing system and interaction between clay layers and host polymer, melt intercalation, solution blending, and in situ polymerization have been used to prepare the nanocomposite [11]. The latter consists of polymerization of monomer in the presence of clay layers. In situ polymerization almost results in the exfoliated structure due to the low viscosity of monomer, which brings about the easy intercalating of monomers into interlayer gallery of clay particles. Because of a variety of polymerization systems and methods, in situ polymerization is

Electronic supplementary material The online version of this article (doi:10.1007/s10965-014-0593-2) contains supplementary material, which is available to authorized users.

M. Farrokhi · M. Abdollahi (✉)
Polymerization Engineering Department, Faculty of Chemical Engineering, Tarbiat Modares University,
P.O. Box: 14115-114, Tehran, Iran
e-mail: abdollahim@modares.ac.ir

one of the most interesting techniques for preparation of the nanocomposite.

Development of controlled radical polymerization (CRP) for synthesis of polymers with controlled architecture, molecular weight, and narrow molecular weight distribution is among the most significant accomplishments in the polymer chemistry. Among the known types of CRP methods, reverse iodine transfer polymerization (RITP) has emerged as an easy, efficient and robust method of CRP, applicable to a wide range of monomers and compatible with both homogeneous and heterogeneous processes. A review of related literatures indicates that most of the vinyl monomers have been polymerized by this method [12–17]. However, few studies have been done on the preparation of nanocomposites by this technique. Optical-functional diblock copolymer brushes grafted from hollow sphere surface have been synthesized by surface-initiated RITP [18]. A sufficient amount of azo initiator was introduced onto the hollow sphere surface firstly. Then, methyl methacrylate was polymerized via surface initiated RITP by using azo group-modified hollow sphere as initiator. Vinylated silica nanoparticles has been modified by radical addition of 1,4-diiodoperfluorobutane initiated by *tert*-butylperoxypivalate, leading to silica with -C_4F_8I end-groups on its surface [19]. Then, the "grafting from" iodine transfer radical polymerization (ITP) of vinylidene fluoride (VDF) initiated by bis(4-*tert*-butylcyclohexyl) peroxydicarbonate from such iodinated silica (Silica-C_4F_8-I) led to silica core/ PVDF shell polymeric nanoparticles.

To our knowledge, there is no report on use of nanoclay in the ITP and RITP reactions to prepare polymer/ clay nanocomposites. In the our previous works [17, 20], copolymers of vinyl acetate (VAc) and dibutyl maleate (DBM) were successfully synthesized by ITP and RITP. In the present work, copolymerization of VAc and DBM via RITP at 70 °C is performed in the presence of various loading amounts of sodium montmorillonite (Na-MMT). Moreover, effect of loading amount of Na-MMT and initial molar ratio of iodine relative to the monomers on the conversion, copolymerization rate, molecular weight and its distribution and nanocomposite structure is investigated by ^{1}H-NMR, GPC and XRD and TEM analyses, respectively.

Experimental

Materials

VAc (Fluka, ≥99 %) and DBM (Merck, for synthesis) monomers were dried with calcium hydride (Merck) under magnetic stirring for 12 h, distilled under vacuum and then stored at −4 °C. I_2 molecule (Merck) was used as an in situ CTA generator without further purification. AIBN (Fluka, ≥98 %) initiator was recrystallized from methanol. n-Hexane (Kiyan Kaveh Azma Co., Iran) were used as received. Na-MMT (from Southern Clay Products Co. with a cation exchange value of 92 meq/100 g) was dried in an oven under vacuum at 60 °C.

Copolymerization of VAc and DBM in the presence of Na-MMT

A required amount of nanoclay and comonomers (VAc and DBM) was introduced into the glass tubes equipped with a magnetic stirrer and rubber septum (Table 1). The glass tubes were degassed by purging the nitrogen into the glass tubes for 30 min and then sealed with a rubber septum. Nanoclay was allowed to disperse in the solution of comonomers with continuous stirring for 3 h at room temperature. Required amounts of AIBN and I_2 were then added to the glass tubes. The final reaction mixture was further degassed by purging the nitrogen for 20 min, sealed with a rubber septum and then immerged in a preheated oil batch at a desired temperature (i.e. 70±0.1 °C). Polymerization was allowed to proceed in the dark while reaction mixture was mixed with the magnetic stirrer. The tube was removed from the oil batch at the given time interval and reaction mixture was immediately immerged in the water/ice batch to stop the reaction. After adding small amount of the hydroquinone as an inhibitor to the reaction mixture, a fraction of that was dried and used in the thermogravimetry analysis (TGA), X-ray diffraction (XRD) and transmission electron microscopy (TEM) analyses. The remained mixture was centrifuged in 20,000 rpm and polymer was separated from Na-MMT. Separated polymer was used in the ^{1}H-NMR and gel permeation chromatography (GPC) analyses.

It should be mentioned that Bulk RITP of VAc and DBM in the absence of Na-MMT has already been performed with a procedure same as that used in the present work [17]. Corresponding results are given in Table 1 for comparison.

Characterization

Individual and overall conversions of the comonomers as well as the copolymer composition were calculated from ^{1}H-NMR spectroscopy recorded by using 500 MHz ^{1}H-NMR spectroscope (500 MHz Bruker) at the ambient temperature. $CDCl_3$ was used as a solvent. Apparent molecular weight and its polydispersity index (PDI) of the polymers dissolved in THF was determined by a Agilent 1,100 gel GPC equipped with a 10^4, 10^3 and 500 A° set of ultrastyragel columns suitable for the molecular weight range of 10^3–10^5 g mol^{-1} and a refractive index (RI) detector. Polystyrene standards with narrow molecular weight distributions and molecular weights in the range of the analyzed molecular weight were used to calibrate the columns. THF was used as an eluent with a flow rate of 1 mL/min at 25 °C. Thermal stability of the nanocomposites

Table 1 ^{1}H-NMR and GPC results for RICTP of VAc and DBM in the absence and presence of Na-MMTat 70 °C

Sample[a]	Time (hr)	$[M]_0/[AIBN]_0/[I_2]_0$	$X_{VAc}/X_{DBM}/X(\%)$[b]	MMT (wt%)[c]	$\overline{F}^b_{VAc}$	$\overline{M}_{n,th}/\overline{M}^*_{n,th}(g/mol)$[d]	$\overline{M}_{n,GPC}(g/mol)$[e]	PDI[e]
V[f]	4	60/1/0.2	77.1/0/0	0	1	9500/7010	8260	
VD1[f]	4	60/1/0.2	69.4/100/72.2	0	0.870	11390/8180	8010	1.64
VD2[f]	4	60/1/0.3	81.1/100/82.7	0	0.889	8600/6960	9820	1.54
VD3[f]	8	60/1/0.4	69.0/100/71.8	0	0.869	5810/4280	5850	1.63
VD4[f]	4	100/1/0.2	69.3/100/72.1	0	0.870	18940/13510	12630	1.83
VD5[f]	4	100/1/0.3	76.6/100/78.8	0	0.887	13640/11070	19330	1.25
VD6[f]	5.5	100/1/0.4	69.2/100/72.0	0	0.862	9560/7820	9160	1.7
VDM2–1	7.5	100/1/0.3	37.5/87.7/42.1	2	0.781	13600/8920	–	–
VDM2–2	8.5	100/1/0.3	45.6/92.2/49.8	2	0.835	13600/8550	–	–
VDM2–3	11	100/1/0.3	59.2/99.6/62.9	2	0.847	13600/7900	7577	1.98
VDM5	70	100/1/0.3	1.2/20.3/2.9	5	0.371	13600/6400	<1000	–
VDM2	11	100/1/0.4	69.4/100.0/72.2	2	0.875	10200/6660	8651	1.76
VDM5	31.5	100/1/0.4	2.2/23.0/4.0	5	0.485	10200/5670	<1000	–

[a] Mole fraction of VAc in initial feed (f^0_{VAc}) was 0.909 ($[VAc]_0/[DBM]_0$=10/1) for all reactions expect for sample V (VAc homopolymerization). Abbreviations of V,D and M in the samples code indicate VAc, DBM and Na-MM respectively

[b] Calculated from ^{1}H NMR spectra via Eqs. (1)–(4)

[c] Weight percent of Na-MMT relative to the total weight of comonomers

[d] Calculated theoretically by using Eqs. (5) and (7)

[e] Obtained from GPC analysis. Samples VDM2–1 and VDM2–2 were not subjected to GPC analysis. For Samples VDM5 and VDM5', accurate PDI could not be obtained by GPC analysis due to their low molecular weights

[f] Experiments reported in the Ref [17]

was investigated by TGA (Mettler, SDTA 851 model) under N_2 atmosphere with a heating rate of 10 °C/min in the temperature range of 25–700 °C. X-ray diffraction spectra were collected on an X-ray diffraction instrument (Siemens D5000) with a Cu K_α radiation (λ=0.154 nm) at the room temperature. The system consists of a rotating anode generator operated at 35 kV and 20 mA current. The samples were scanned from 2θ=2 to 10° at the step scan mode, and the diffraction pattern was recorded using a scintillation counter detector. The distribution of clay layers into the polymer matrix was studied by using a TEM (Philips) operated at an accelerated voltage of 300 kV. Nanocomposite samples were diluted with the ethanol and then one drop of the diluted suspensions was suspended on a carbon-coated copper grid, vacuum dried and subjected to TEM observation.

Results and discussion

RITP offers an appealing potential to in situ generate transfer agents out of molecular iodine, I_2. This method is employed in the present work to synthesize P(VAc-co-DBM)/ clay nanocomposites. General procedure of the copolymerization of VAc and DBM in the presence of Na-MMT and I_2 initiated with AIBN is shown in Scheme 1.

Figure 1 shows typical ^{1}H-NMR spectrum of the reaction mixture containing the unreacted comonomers and produced copolymer separated from Na-MMT at the overall molar conversion of 42.1 % for bulk iodine transfer radical copolymerization (RITCP) of VAc and DBM (VDM2-1, Table 1). All peaks appeared in the ^{1}H-NMR spectrum were assigned to the corresponding protons (Fig. 1) [17, 20]. A very small portion of the chain ends with iodinated VAc has been reported to degrade to the aldehyde groups during the reaction [20, 21]. Proton of the aldehyde groups appears at the chemical shift of about 9.6–9.9 ppm (Fig. 1). By neglecting these aldehyde groups, it is possible from ^{1}H-NMR spectrum to calculate individual conversion of the VAc (X_{VAc}) and DBM (X_{DBM}) via Eqs. (1) and (2), respectively.

$$X_{VAc} = \frac{I_{(b+c')} - I_a}{I_{(b+c')}} \quad (1)$$

$$X_{DBM} = \frac{I_{(m+m')} - (3 \times I_e)}{I_{(m+m')}} \quad (2)$$

in which I_i indicate the peak intensity of proton(s) i. Then, overall conversion of the comonomers (X) and cumulative mole fraction of VAc incorporated into the copolymer chain

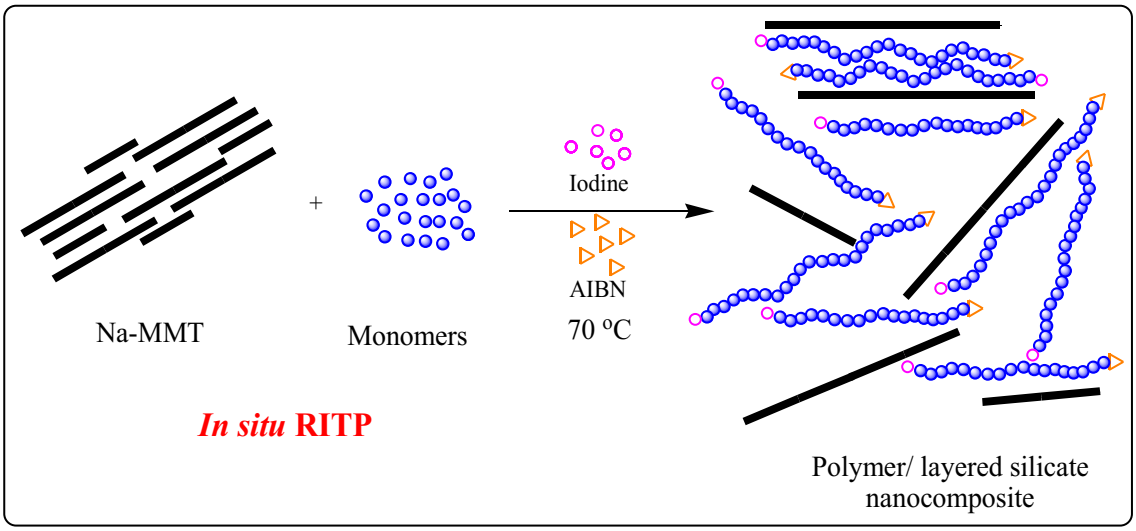

Scheme 1 Schematic presentation of the general procedure for preparation of polymer/ Na-MMT nanocomposite via RITP in the presence of Na-MMT

$(\overline{F}_{VAc})$ at any time can be calculated by using Eqs. (3) and (4), respectively.

$$X = f^0_{VAc}X_{VAc} + f^0_{DBM}X_{DBM} \tag{3}$$

$$\overline{F}_{VAc} = \frac{\frac{n^0_{VAc}}{n^0_{DBM}}X_{VAc}}{\frac{n^0_{VAc}}{n^0_{DBM}}X_{VAc} + X_{DBM}} \tag{4}$$

in which f^0_{VAc} and f^0_{DBM} are mole fraction of the comonomers of VAc and DBM in the initial feed, respectively, and n^0_{VAc} and n^0_{DBM} indicate mole of comonomers VAc and DBM in the initial reaction mixture, respectively.

Theoretical number-average molecular weight $(\overline{M}_{n,th})$ in the RITP reaction can be estimated by Eq. (5).

$$\overline{M}_{n,th} = \sum_{i=1}^{n}\left(\frac{[M_i]_0X_iM_{w,i}}{2[I_2]_0}\right) + M_{A\text{–}I} \tag{5}$$

in which $[M_i]_0$ indicates initial concentration of the comonomer i. $M_{w,i}$ is molecular weight of the comonomer i (86.09 and 228.29 $g.mol^{-1}$ for VAc (i=1) and DBM (i=2) respectively), X_i indicates molar conversion of the comonomer i and $M_{A\text{–}I}$ illustrates molecular weight of the α and ω nd groups of the polymer chain ($M_{A\text{–}I}$=195 $gmol^{-1}$ in the present case) originated from initiator-derived radical fragment (A = $(CH_3)_2(CN)C$-) and iodine molecule (–I).

Growing chains generated from excess initiator during the propagation step of the RITP have not been considered in Eq. (5). Moreover, Since there is an inhibition period in the RITP reaction, hence, Eq. (5) should be revised by considering the inhibition period time (t_{inh}) and AIBN concentration at the end of inhibition period ($[AIBN]_{t,inh}$) where there is no free I_2 to react with the initiator- derived radicals. Consequently, more accurate value of the theoretical $\overline{M}_n$, i.e. $\overline{M}^*_{nth}$, in RITP can be calculated by Eq. (7).

$$[AIBN]_{t,inh} = [AIBN]_0\exp(-k_dt_{inh}) \tag{6}$$

$$\overline{M}^*_{n,th} = \sum_{i=1}^{n}\left(\frac{[M_i]_0X_iM_{w,i}}{2[I_2]_0 + [AIBN]_{t,inh}f(1-e^{-k_d\tau})}\right) + M_{A\text{–}I} \tag{7}$$

in which $[AIBN]_0$ and $[AIBN]_{t,inh}$ indicate concentration of the AIBN at the beginning of the reaction and end of the inhibition period, respectively. t and τ are the reaction time and reduced reaction time τ (=t−t_{inh}). k_d and f indicate the decomposition rate constant (k_d=3.166 × $10^{-5}s^{-1}$ at 70 °C) and efficiency (f=0.7) [22] of the AIBN initiator, respectively.

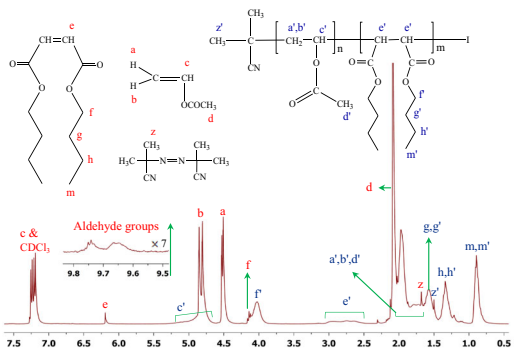

Fig. 1 ^{1}H-NMR spectrum of the reaction mixture containing the unreacted comonomers and produced copolymer separated from nanoclay after the overall monomers conversion of 42.1 mole % for bulk RITCP of VAc and DBM in the presence of 2 wt% Na-MMT with $[M]_0$:$[AIBN]_0$:$[I_2]_0$=100:1:0.3 at 70 °C (sample VDM2-1 in Table 1)

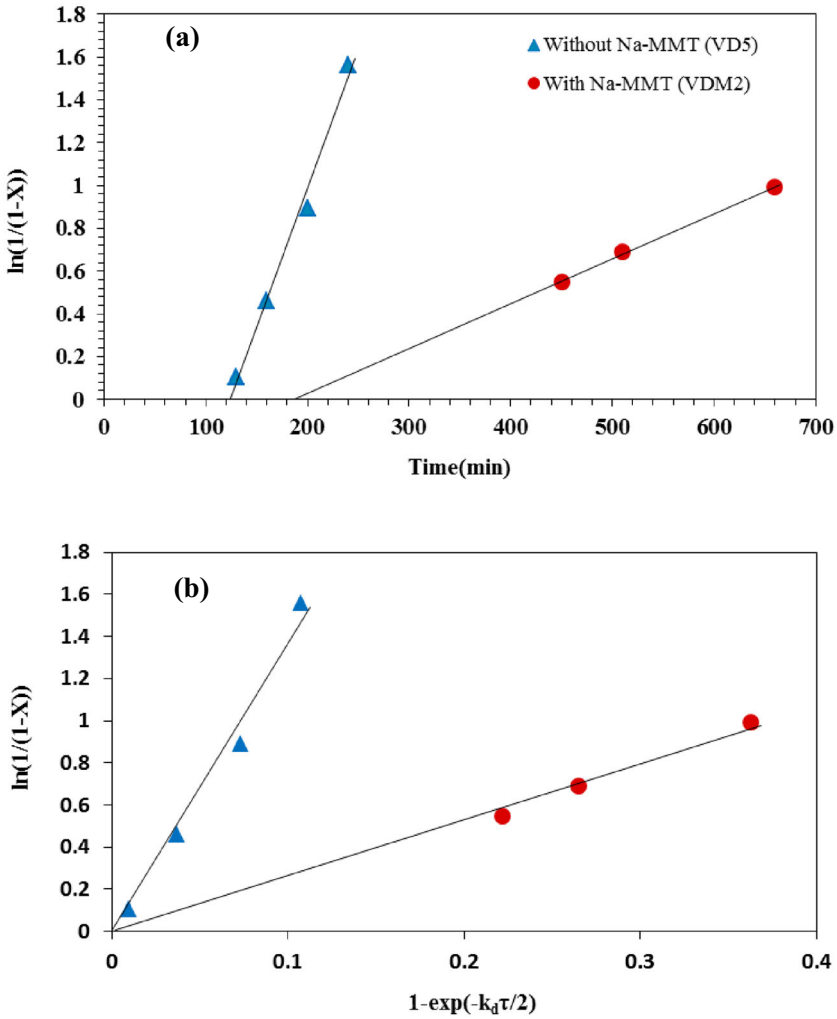

Fig. 2 Effect of nanoclay on the ln(1/(1-X)) versus time (**a**) and ln(1/(1-X)) versus [1-exp(−$k_d\tau$/2)] (**b**) for the RITCP of VAc and DBM at 70 °C (Table 1)

A summary of results obtained from GPC and ^{1}H-NMR analyses for RITCP of VAc and DBM in the absence and presence of Na-MMT is given in Table 1. There is a relatively good agreement between the $\overline{M}_{n,GPC}$ and theoretical $\overline{M}_n$ (i.e., $\overline{M}_{n,th}$ or $\overline{M}^*_{n,th}$). As expected from Eqs. (5) and (7), in the RITCP of VAc and DBM without Na-MMT, molecular weight of the copolymer increases at the same conversion by increasing the initial concentration of monomers relative to those of AIBN and I_2 (for example see samples VD3 and VD6 in Table 1) as well as by decreasing the initial concentration of I_2 relative to the monomers (VD1 and VD3 in Table 1). By considering the AIBN efficiency (f=0.7), the best result was obtained with I_2 to AIBN initial molar ratio of 0.3 to 1 (VD5) where higher conversion and highest molecular weight with the minimum PDI of the molecular weight, i.e. PDI=1.25, was obtained.

However, different behavior was observed in RITCP of VAc and DBM in the presence of Na-MMT. It is clear from Table 1 that unlike the RITCP of VAc and DBM without Na-MMT, conversion and thereby molecular weight of the copolymer increased at the same reaction time by increasing the molar percentage of the iodine relative to the monomers in initial mixture from 0.3 to 0.4 in the presence of Na-MMT (samples VDM2-3 and VDM2′)(see Fig. S1 in the supporting information). This behavior indicates that functional groups in the clay's surface may react with the monomers and iodine [23–25]. It was observed from color of the reaction mixture that a portion of iodine always interact with functional groups in the clay's surface and does not participate in the reaction, resulting in the $\overline{M}_{n,GPC}$ alue higher than that of $\overline{M}^*_{n,th}$ in the case of VDM2' (Table 1). Moreover, by increasing the loading of nanoclay from 2 to 5 wt%, conversion and thereby molecular weight decreased (samples VDM5 and VDM5′). It may be attributed to undesirable chain transfer reactions in the presence of nanoclay.

Interaction between the hydroxyl groups (Al-O-H) present in the surface of nanoclay and carbonyl group of the monomers such as VAc, methyl methacrylate [23] and ethyl acrylate

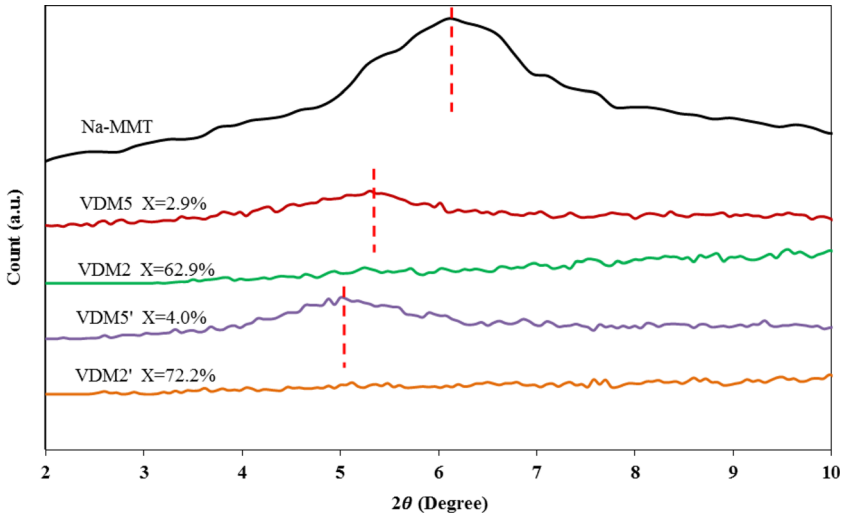

Fig. 3 XRD patterns of the neat Na-MMT and P(VAc-co-DBM)/ Na-MMT nanocomposites with various Na-MMT loading amounts

[24] has been observed. It has been reported that use of nanoclay in the atom transfer radical polymerization of the above- mentioned monomers leads to a significant increase in the homopolymerization rate. It is clear from Table 1 that copolymer composition $\left(\overline{F}_{VAc}\right)$ at the same conversion is slightly different for reactions performed without and with Na-MMT (VD6 and VDM2' respectively). Moreover, PDI of the molecular weight of the produced copolymers increases in the presence of Na-MMT. It can be attributed to existence of an interaction between the monomers and nanoclay as well as to undesirable chain transfer reactions in the presence of nanoclay [22–25].

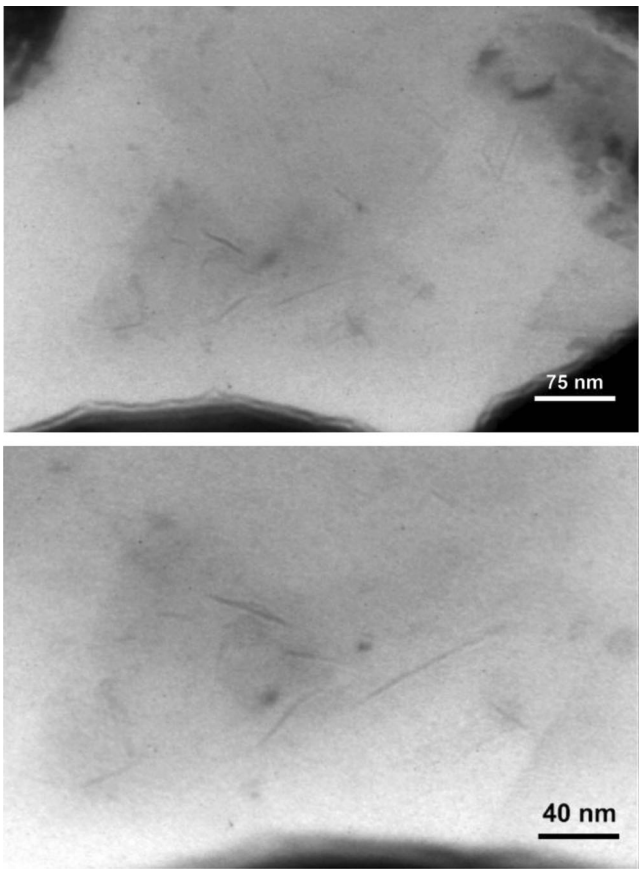

Fig. 4 TEM micrograph of the P(VAc-co-DBM)/ Na-MMT nanocomposite of sample VDM2–3

Figure 2(a) shows the plots of ln(1/(1-X)) versus time for RITCP of VAc and DBM with and without Na-MMT. As mentioned earlier, data related to RITCP of VAc and DBM in the absence of Na-MMT have already been reported [17]. It is clear from Fig. 2(a) that dependence of ln(1/(1-X)) on time is linear for both copolymerization systems, indicating that radical concentration is constant throughout the reaction and R_p is also proportional with the first order of the comonomers concentration. In addition, in presence of nanoclay, polymerization rate decreases while the inhibition period time increases. It means that nanoclay can act as both inhibitor and retarder in the RITCP of VAc and DBM, indicating again that nanoclay may interact with I_2 and comonomers [26, 27]. Retardation effect of the nanoclay via chain transfer reactions may result in the decreased molecular weights as can be seen in Table 1.

In the free-radical polymerization, rate of polymerization is dependent on the lumped kinetic parameter (i.e. $k_p k_t^{-0.5}$) via the following equation [28].

$$\ln\left(\frac{1}{1-X}\right) = 2k_p\left(\frac{f[AIBN_0]}{k_d k_t}\right)^{0.5}(1-\exp(-k_d t/2)) \qquad (8\text{–}1)$$

in which k_p and k_t are average propagation and termination, respectively, rate constant of (co) polymerization reaction. In the RITP reaction, however, there is an inhibition time to be considered in the Eq. (8–1). Then, Eq. (8–1) can be rewritten as Eq. (8–2) which is useful for RITP [17].

$$\ln\left(\frac{1}{1-X}\right) = 2k_p\left(\frac{f[AIBN]_{t,inh}}{k_d k_t}\right)^{0.5}(1-\exp(-k_d \tau/2)) \quad (8\text{–}2)$$

By considering k_d and f values of AIBN at 70 °C ($3.166 \times 10^{-5}\,s^{-1}$ and 0.7, respectively) [22], $k_p k_t^{-0.5}$ value for RITCP

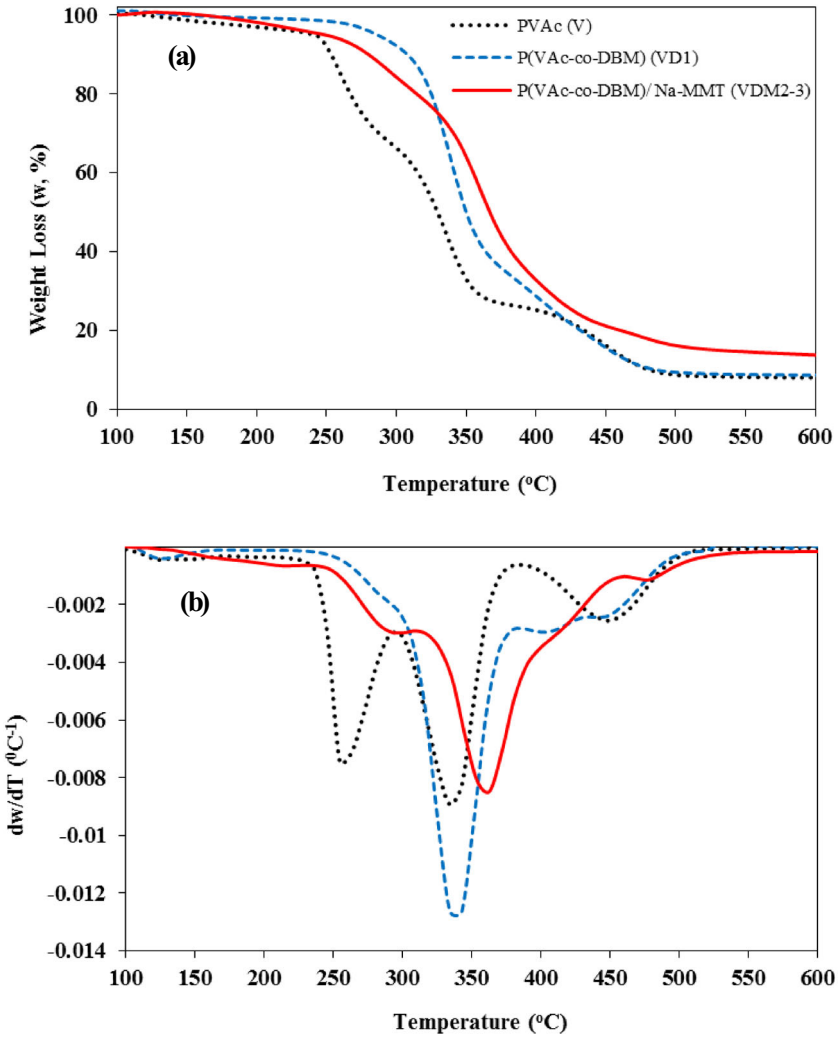

Fig. 5 TGA (**a**) and DTG (**b**) thermograms obtained for PVAc (sample V), P(VAc-co-DBM) copolymer (sample VD1) and P(VAc-co-DBM)/ Na-MMT nanocomposite (sample VDM2–3) synthesized by RITP at 70 °C

of VAc and DBM in the absence and presence of the Na-MMT with f^0_{VAc} of 0.909 was calculated from slope of ln(1/(1-X)) versus (1-exp($-k_d\tau/2$) plots (Fig. 2(b)) to be 2.35×10^{-1} and $4.85 \times 10^{-2} L^{0.5}$ $mol^{-0.5}$ $s^{-0.5}$, respectively. It is clear that $k_p k_t^{-0.5}$ value and thereby copolymerization rate decreases one order of magnitude in the presence of nanoclay.

Figure 3 shows XRD patterns for neat Na-MMT and VAc/DBM nanocomposites containing nanoclay loading of 2 wt% (samples VDM2-3 and VDM2′) and 5 wt% (samples VDM5 and VDM5′). It is clear from Fig. 3 that in the samples with 5 wt% nanoclay loading where conversion of comonomers is very low, there is a basal spacing (d_{001}) peak which has been shifted to the lower angle in comparison with that of the neat Na-MMT, indicating formation of the intercalated structure. Moreover, by increasing overall conversion of the comonomers from 2.9 mol% for sample VDM5 to 4.0 mol% for sample VDM5′, this peak shifts to a lower angle, demonstrating that gallery spacing of the nanoclay increases. On the other hand, in VDM2–3 and VDM2′ with 2 wt% nanoclay and higher comonomers conversion, there is no peak in the range of 2θ=2–10°, suggesting that exfoliated structure may also be formed.

Table 2 Data on the thermal stability of the homo-and copolymers of VAc and DBM

Sample	$T_{d,5\%}$(°C)	Residual weight at 600 °C (wt%)	$T_{d,max}$(°C)
V	237	7.963	334
VD1	283	8.617	343
VDM2–3	248	13.583	363

To further investigate structure of the nanocomposites, the sample VDM2–3 was subjected to the TEM analysis and the corresponding micrograph is shown in Fig. 4. The clay layers appear as dark strips while the polymer matrix appears as a gray/white domain. It is clear from this image that silicate layers are disordered, dispersed, and well delaminated with a thickness of about 1.9–4 nm in the polymer matrix, indicating that both exfoliated and intercalated morphology may be formed.

TGA and derivative thermogravimetry (DTG) curves related to the PVAc homopolymer (Sample V), P(VAc-co-DBM) copolymer (sample VD1) and P(VAc-co-DBM)/ Na-MMT nanocomposite (sample VDM2–3) synthesized by using RITP are shown in Fig. 5. For samples subjected to TGA analysis, temperatures related to 5 wt% degradation ($T_{d,5\%}$) and maximum degradation rate ($T_{d,max}$) along with the residual weight at 600 °C are also given in Table 2. Degradation of PVAc starts at about 225 °C. The first step of PVAc degradation occurs at about 225–375 °C, which can be attributed to the removal of the acetoxy groups, resulting in a polyene backbone. In the second step (about 385–500 °C), the polyene rearranges and degrades to aromatic and aliphatic hydrocarbons [20, 29, 30]. Obviously, it can be seen from TGA and DTG thermograms that presence of DBM in the VAc/DBM copolymer increases their thermal stability with maximum degradation rate at 343 °C (Table 2). Moreover, presence of the Na-MMT in the VAc/DBM copolymer increases its thermal stability with a maximum degradation rate at 363 °C (Table 2). The enhanced char yield can also been seen in the presence of nanoclay (Table 2). It should be noted that the char residue formation usually governs flammability behavior of the nanostructured materials (Fig. 5).

Conclusion

RITP as an method to in situ generate transfer agent from molecular I_2 in the presence of initiator was successfully employed to synthesize P(VAc-co-DBM) and its nanocomposites with Na-MMT in the bulk at 70 °C. ^{1}H-NMR and GPC results showed that products with predetermined molecular weight can be synthesized by this method in the presence of Na-MMT. It was found in the RITCP of VAc and DBM in the presence of Na-MMT that molecular weight decreases significantly by increasing Na-MMT content and conversion limits to a very low value when 5 wt% clay loading is used. Moreover, by increasing the initial molar percentage of iodine relative to the monomers from 0.3 to 0.4, molecular weight and conversion increased and PDI of the molecular weight decreased while opposite behavior has been observed for RITP of VAc/DBM in the absence of Na-MMT. $k_p k_t^{-0.5}$ value in the copolymerization system with f^0_{VAc} of 0.909 decreased from $2.353 \times 10^{-1} L^{0.5} mol^{-0.5} s^{-0.5}$ in the absence of Na-MMT to $4.85 \times 10^{-2} L^{0.5} mol^{-0.5} s^{-0.5}$ in the presence of Na-MMT. It was concluded from kinetic study that nanoclay can play as both inhibitor and retarder in the RITP of VAc and DBM. All observations suggest existence of the undesirable transfer reaction in the presence of clay as well as existence of the interactions between the nanoclay and I_2 or monomers. In comparison with results obtained for reactions at low conversion, XRD and TEM results showed that better dispersion of the clay in the polymer matrix can be obtained only when the reaction proceeds up to the high conversion where the polymer chains grow up to the relatively high lengths.

References

1. Fu X, Qutubuddin S (2001) Polymer 42:807–813
2. Rahimi-Razin S, Salami-Kalajahi M, Haddadi-Asl V, Roghani-Mamaqani H (2012) J Polym Res 19:1–16
3. Pavlidou S, Papaspyrides CD (2008) Prog Polym Sci 33:1119–1198
4. Sinha Ray S, Okamoto M (2003) Prog Polym Sci 28:1539–1641
5. Fujimori A, Ninomiya N, Masuko T (2008) Polym Adv Technol 19: 1735–1744
6. Caruso F, Spasova M, Susha A, Giersig M, Caruso RA (2000) Chem Mater 13:109–116
7. Jang BN, Costache M, Wilkie CA (2005) Polymer 46:10678–10687
8. Nazarenko S, Meneghetti P, Julmon P, Olson BG, Qutubuddin S (2007) J Polym Sci Polym Phys 45:1733–1753
9. Shia D, Hui CY, Burnside SD, Giannelis EP (1998) Polym Compos 19:608–617
10. Tao Y, Endo M, Inagaki M, Kaneko K (2011) J Mater Chem 21:313–323
11. Wang D, Zhu J, Yao Q, Wilkie CA (2002) Chem Mater 14:3837–3843
12. Boyer C, Lacroix-Desmazes P, Robin J-J, Boutevin B (2006) Macromolecules 39:4044–4053
13. Lacroix-Desmazes P, Severac R, Boutevin B (2005) Macromolecules 38:6299–6309
14. Rayeroux D, Patra BN, Lacroix-Desmazes P (2013) J Polym Sci Polym Chem 51:4389–4398
15. Wright T, Chirowodza H, Pasch H (2012) Macromolecules 45:2995–3003
16. Xu W, Zhang W, Li W, Yan J, Shen G, Li J (2012) J Appl Polym Sci 126:104–109
17. Farrokhi M, Abdollahi M (2014) Iran J Polym Sci Technol (Accepted)
18. Wang L-P, Dong L-H, Hao J-C, Lv X-H, Li W-Z, Li Y-C, Zhen J-M, Hao Y-C, Ma F (2011) J Colloid Interface Sci 361:400–406
19. Durand N, Boutevin B, Silly G, Améduri B (2011) Macromolecules 44:8487–8493
20. Farrokhi M, Abdollahi M, Hemmati M (2014) Polym Int 63:1494–1504
21. Iovu MC, Matyjaszewski K (2003) Macromolecules 36:9346–9354
22. Matheson MS, Auer EE, Bevilacqua EB, Hart EJ (1949) J Am Chem Soc 71:2610–2617
23. Krishna BS, Selvaraj S, Mohan BV, Murty DSR, Jai Prakash BS (1998) Bull Mater Sci 21:355–361
24. Bosco JWJ, Agrahari A, Saikia AK (2006) Tetrahedron Lett 47: 4065–4068
25. Riebe B, Dultz S, Bunnenberg C (2005) Appl Clay Sci 28:9–16
26. Abdollahi M, Semsarzadeh MA (2009) Eur Polym J 45:985–995
27. Datta H, Singha NK, Bhowmick AK (2007) Macromolecules 41:50–57
28. Semsarzadeh MA, Abdollahi M (2008) J Appl Polym Sci 110:1784–1796
29. Rimez B, Rahier H, Van Assche G, Artoos T, Biesemans M, Van Mele B (2008) Polym Degrad Stab 93:800–810
30. Vasile C, Cascaval CN, Barbu P (1981) J Polym Sci: Polym Chem Ed 19:907–916